PICO-60 Results and PICO-40L Status

C. B. Krauss[1] for the PICO Collaboration

[1]Department of Physics, University of Alberta, Edmonton, T6G 2E1, Canada

E-mail: analysis@picoexperiment.com

Abstract. PICO-60 and PICO-40L are bubble chambers for dark matter searches that are using C_3F_8 as active liquid. PICO-60 was operated successfully at SNOLAB until 2017 and PICO-40L is now operating in the same location. PICO-40L follows a new detector concept that holds promise for future increases of sensitivity. We present the projected sensitivity of PICO-40L for the WIMP-proton cross section.

1. PICO-60 Results

The PICO experimental programme for dark matter search with superheated Freon has led to large improvements in sensitivity over the past 7 years, since the PICO collaboration was formed. The PICO-60 detector was operated with 52 kg of active C_3F_8 from 2016 to 2017. We have recently reported the analysis results of the complete exposure of the PICO-60 data, that combines the data from the first month of blind data taking at 3.3 keV threshold [1] with the data from the second month of data taking with a threshold of 2.45 keV. These two data sets were analyzed with the most recent threshold data extracted from PICO calibration runs [2] to give a new world leading result for spin dependent WIMP proton interactions shown in figure 1. The improvements compared to the first PICO-60 paper [1] are from the lower threshold data and show the potential of the bubble chamber technique at lower thresholds. The full discussion of the new results can be found in [3].

2. PICO-40L Status

PICO-60 was decommissioned after the data taking was complete in 2017 to make room for the PICO-40L experiment that eliminates the buffer liquid from direct contact with the clean active liquid. This change in the detector operation requires several changes in the way the detector is designed:

(i) The active liquid needs to be kept in a synthetic quartz jar, just as before. But the seals with the stainless steel bellows will be required to be kept below the boiling point of the active liquid so that spurious boiling at the seals is prevented.

(ii) In order to keep the cold liquid at the seals from mixing with the superheated liquid, the seals need to be at the bottom of the active liquid, requiring the detector to be turned upside down with respect to the previous detector generation. We refer to this detector geometry as "right-side-up", shown in figure 2. The performance of this type of chamber was recently verified in [4].

(iii) The bellows that allows the pressure differential between the surrounding hydraulic liquid and the active liquid to be kept small is a source of steel particulate matter. The right side

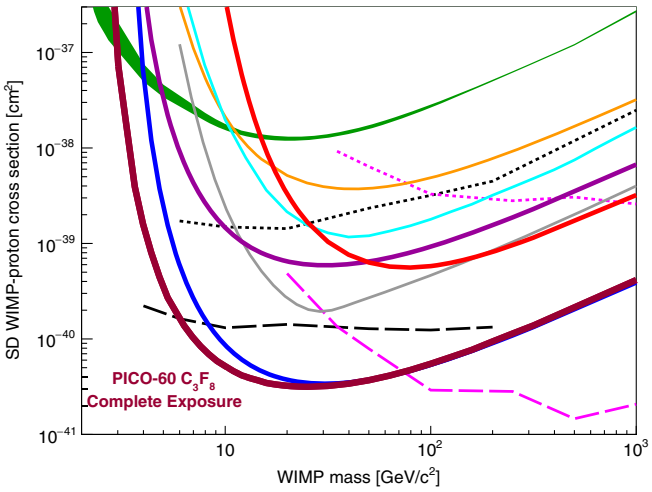

Figure 1. Updated exclusion limit from PICO-60 as reported in [3]. The lowest line shows the limit PICO-60 was able to exclude at 90% C.L. using the complete exposure. The 90% C.L. limit on the SD WIMP-proton cross section from the profile likelihood analysis of the PICO-60 C_3F_8 combined blind exposure plotted in thick maroon, along with limits from the first blind exposure of PICO-60 C_3F_8 (thick blue) [1], as well as limits from PICO-60 CF_3I (thick red) [5], PICO-2L (thick purple) [6], PICASSO (green band) [7], SIMPLE (orange) [8], XENON1T (gray) [9], PandaX-II (cyan) [10], IceCube (dashed and dotted pink) [11], and SuperK (dashed and dotted black) [12, 13]. The indirect limits from IceCube and SuperK assume annihilation to τ leptons (dashed) and b quarks (dotted).

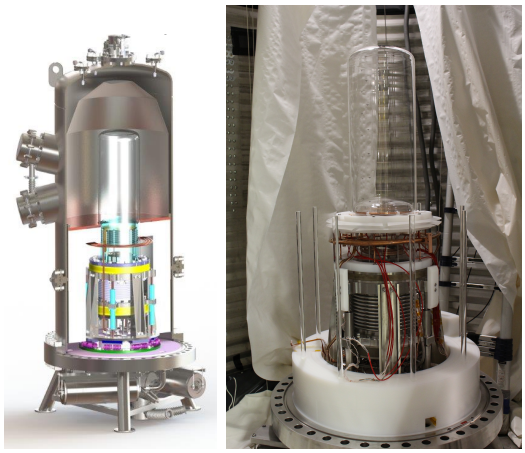

Figure 2. left side: schematic view of the PICO-40L detector. The HDPE thermal insulation between the pressure vessel and the inner detector assembly is visible in white. Cooling coils are outside and inside the quartz jars nested inside another. Right side: view of the inner detector during assembly.

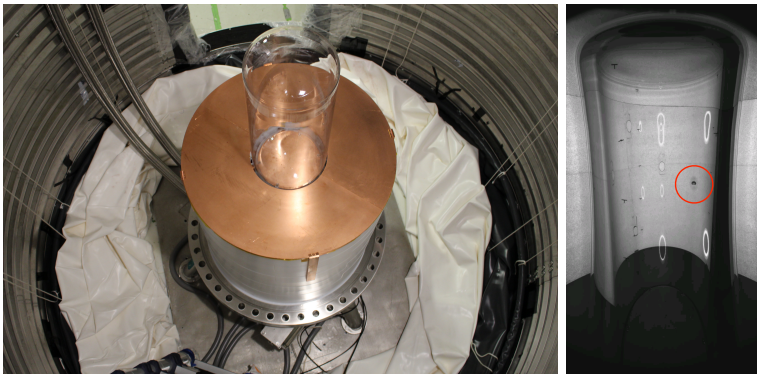

Figure 3. Left side: View from the top showing the assembled inner vessel section of the PICO-40L experiment. Right side: one of the first bubbles recorded with PICO-40L, bubble highlighted by a red circle.

up detector geometry helps to deal with these particulates by allowing them to permanently settle in the cold, inactive region of the detector.

The full geometry of the PICO-40L detector is shown in figure 2. The size and design of the quartz vessel is identical to one used in the previous PICO-60 detector, but the bellows component is now below the active mass and thermally isolated from the superheated temperature (usually between 14 °C and 16 °C in C_3F_8). The new detector also has a much improved clearance between the central quartz vessel and the stainless steel pressure vessel surrounding it. PICO-60 was ultimately limited by the backgrounds created from the steel pressure vessel and therefore could not be operated at lower thresholds or for longer times. PICO-40L addresses this limitation by increasing the amount of hydraulic fluid that also serves as neutron shield separating the active liquid from the mechanical and optical components of the detector.

In order to operate PICO-40L stably the area around the glass to steel seals is kept below –35 °C while the detector itself is kept warm. This requires a new thermal control system that chills the hydraulic liquid at the bottom and a system of heaters that warm up the active part of the detector. All components of the new detector were cleaned, assembled and the detector was filled with active and hydraulic liquid in spring 2019. Currently the detector is undergoing commissioning to determine the most stable operational set points and optimal trigger and running conditions. The first bubbles have been observed, but it is too soon to make statements about the radon induced alpha background level and surface event rates at this point.

PICO-40L will ultimately reach the sensitivity for spin dependent WIMP proton interactions after a year of running, as shown in figure 4. Note that this is exploring parameter space that is below the WIMP neutrino elastic scattering background level from coherent solar neutrino-nucleus interactions on xenon.

3. Summary

In summary PICO-40L and PICO-60 have been milestones in the development of dark matter detection with superheated liquids. The most recent PICO-60 data at 3.3 keV was background free and PICO-40L is designed to be background free for a yearlong exposure. Next, the PICO collaboration is pursuing the PICO-500 experiment that will push the sensitivity level of dark matter experiments with fluorine as target by another order of magnitude to reach a sensitivity that allows the observation of the coherent neutrino nucleus scattering also with fluorine.

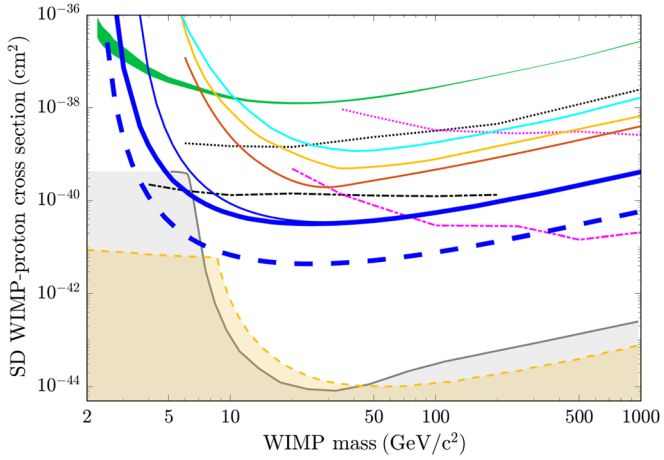

Figure 4. Projected 90% C.L. spin-dependent WIMP-proton exclusion [14] (dashed blue line) for two expected background events in PICO-40L at a 2.8 keV threshold with 1.64 $\times 10^4$ kg-days of exposure, as compared against existing limits from PICO-60 (solid blue line) [1, 3], XENON1T (orange line) [9], LUX (yellow line) [17], PandaX-II (cyan line) [10], and PICASSO (green line) [7]. Indirect limits from IceCube (magenta) [11] and SuperK (black) [13] are also shown assuming annihilation to τ leptons (dotted lines) and b quarks (dashed-dotted lines). The coherent elastic neutrino-nucleus scattering floors for xenon (spin-dependent neutron, gray shaded) and C_3F_8 (no energy resolution, orange shaded) are determined in [25].

References

[1] C. Amole *et al.*, Phys. Rev. Lett. **118**, 251301 (2017).
[2] M. Jin, Ph.D. thesis, Northwestern University, 2019.
[3] C. Amole *et al.*, Phys. Rev. D **100**, 022001, (2019).
[4] M. Bressler *et al.*, 2019 JINST 14 P08019
[5] C. Amole *et al.*, Phys. Rev. D **93**, 052014, (2016).
[6] C. Amole *et al.*, Phys. Rev. D **93**, 061101 (2016).
[7] E. Behnke *et al.*, Astropart. Phys. **90**, 85 (2017).
[8] M. Felizardo *et al.*, Phys. Rev. D **89**, 072013 (2014).
[9] E. Aprile *et al.*, Phys. Rev. Lett. **122**, 141301 (2019).
[10] C. Fu *et al.*, Phys. Rev. Lett. **118**, 071301 (2017).
[11] M. G. Aartsen *et al.*, Eur. Phys. J. C **77**, 146 (2017).
[12] T. Tanaka *et al.*, Astroph. J. **742**, 78 (2011).
[13] K. Choi *et al.*, Phys. Rev. Lett. **114**, 141301 (2015).
[14] D. Baxter *et al.*, Phys. Rev. D **100**, 082006, (2019).
[15] D. S. Akerib *et al.*, Phys. Rev. Lett. **116**, 161302 (2016).
[16] E. Aprile *et al.*, Phys. Rev. Lett. **121**, 111302 (2018).
[17] D. S. Akerib *et al.*, Phys. Rev. Lett. **118**, 021303 (2017).
[18] A. Tan *et al.*, Phys. Rev. Lett. **117**, 121303 (2016).
[19] R. Agnese *et al.*, Phys. Rev. Lett. **116**, 071301 (2016).
[20] G. Angloher *et al.*, Eur. Phys. J. C **76**, 25 (2016).
[21] E. Aprile *et al.*, Phys. Rev. D **94**, 122001 (2016).
[22] R. Agnese *et al.*, Phys. Rev. Lett. **112**, 241302 (2014).
[23] R. Agnese *et al.*, Phys. Rev. D **92**, 072003 (2015).
[24] L. Hehn *et al.*, Eur. Phys. J. C **76**, 548 (2016).
[25] F. Ruppin, *et al.*, Phys. Rev. D **90**, 083510 (2014).